



OPEN ACCESS

ORIGINAL ARTICLE

HBV infection-induced liver cirrhosis development in dual-humanised mice with human bone mesenchymal stem cell transplantation

Lunzhi Yuan,¹ Jing Jiang,² Xuan Liu,¹ Yali Zhang,¹ Liang Zhang,¹ Jiaojiao Xin,² Kun Wu,¹ Xiaoling Li,¹ Jiali Cao,¹ Xueran Guo,¹ Dongyan Shi,² Jun Li,³ Longyan Jiang,² Suwan Sun,² Tengyun Wang,¹ Wangheng Hou,¹ Tianying Zhang,¹ Hua Zhu,⁴ Jun Zhang,¹ Quan Yuan,¹ Tong Cheng,¹ Jun Li,² Ningshao Xia¹

For numbered affiliations see end of article.

Correspondence to

Associate Professor Tong Cheng, State Key Laboratory of Molecular Vaccinology and Molecular Diagnostics, National Institute of Diagnostics and Vaccine Development in Infectious Diseases, School of Life Sciences and School of Public Health, Xiamen University, Xiamen, 361102, China; tcheng@xmu.edu.cn, Professor Jun Li, State Key Laboratory of Diagnosis and Treatment of Infectious Diseases, Collaborative Innovation Center for Diagnosis and Treatment of Infectious Diseases, The First Affiliated Hospital, Zhejiang University School of Medicine, Hangzhou 310003, China; lijun2009@zju.edu.cn and Professor Ningshao Xia, State Key Laboratory of Molecular Vaccinology and Molecular Diagnostics, National Institute of Diagnostics and Vaccine Development in Infectious Diseases, School of Life Sciences and School of Public Health, Xiamen University, Xiamen, 361102, China; nsxia@xmu.edu.cn

LY, JJ and XL contributed equally.

Received 24 January 2018
Revised 9 November 2018
Accepted 8 December 2018
Published Online First
30 January 2019



© Author(s) (or their employer(s)) 2019. Re-use permitted under CC BY-NC. No commercial re-use. See rights and permissions. Published by BMJ.

To cite: Yuan L, Jiang J, Liu X, et al. *Gut* 2019;68:2044–2056.

ABSTRACT

Objective Developing a small animal model that accurately delineates the natural history of hepatitis B virus (HBV) infection and immunopathophysiology is necessary to clarify the mechanisms of host-virus interactions and to identify intervention strategies for HBV-related liver diseases. This study aimed to develop an HBV-induced chronic hepatitis and cirrhosis mouse model through transplantation of human bone marrow mesenchymal stem cells (hBMSCs).

Design Transplantation of hBMSCs into *Fah^{-/-}Rag2^{-/-}IL-2Rγc^{-/-}SCID* (FRGS) mice with fulminant hepatic failure (FHF) induced by hamster-anti-mouse CD95 antibody JO2 generated a liver and immune cell dual-humanised (hBMSC-FRGS) mouse. The generated hBMSC-FRGS mice were subjected to assessments of sustained viremia, specific immune and inflammatory responses and liver pathophysiological injury to characterise the progression of chronic hepatitis and cirrhosis after HBV infection.

Results The implantation of hBMSCs rescued FHF mice, as demonstrated by robust proliferation and transdifferentiation of functional human hepatocytes and multiple immune cell lineages, including B cells, T cells, natural killer cells, dendritic cells and macrophages. After HBV infection, the hBMSC-FRGS mice developed sustained viremia and specific immune and inflammatory responses and showed progression to chronic hepatitis and liver cirrhosis at a frequency of 55% after 54 weeks.

Conclusion This new humanised mouse model recapitulates the liver cirrhosis induced by human HBV infection, thus providing research opportunities for understanding viral immune pathophysiology and testing antiviral therapies in vivo.

INTRODUCTION

HBV infection, which has a complicated progressive course, is a serious public health problem throughout the world and greatly increases the risk for liver cirrhosis.^{1,2} Immune and inflammatory responses are critical in HBV infection and progression to chronic liver diseases. In the past few years, several animal models (woodchucks, tupaia and human liver chimeric mouse) have been developed for modelling HBV infection, but these animals do not exhibit the full immune response spectrum due to the very

Significance of this study

What is already known on this subject?

- ▶ Host immune and inflammatory responses are critical in HBV infection and progression to end-stage liver cirrhosis, but the mechanism remains unclear, and there is currently no cure for chronic HBV infection.
- ▶ Few liver and immune system dual-humanised mouse models generated by the co-transplantation of human haematopoietic stem cells and hepatocytes can mimic HBV viremia, but the long-term progression of HBV-induced liver cirrhosis has not been obviously observed.
- ▶ Implanted human bone marrow mesenchymal stem cells (hBMSCs) in fulminant hepatic failure animal can efficiently proliferate and transdifferentiate into functional hepatocytes, and such cells may be susceptible to HBV infection. However, whether implanted hBMSCs are capable of differentiation into syngeneic immune cells for responding against HBV needs to be clarified.

What are the new findings?

- ▶ A new liver and immune system dual-humanised ‘hBMSC-*Fah^{-/-}Rag2^{-/-}IL-2Rγc^{-/-}SCID* (FRGS)’ mouse model was developed in mice with fulminant hepatic failure through a single transplantation of hBMSCs.
- ▶ The hBMSCs implanted through one splenic injection of hBMSCs transdifferentiated into functional human hepatocytes and multiple immune cell lineages including B cells, T cells, natural killer cells, dendritic cells and macrophages.
- ▶ The dual-humanised hBMSC-FRGS mice were sensitive to chronic HBV infection, generated sustained human immune and inflammatory responses and ultimately developed liver cirrhosis.

narrow host range of HBV.^{3–6} Although chimpanzees are fully permissive for HBV infection, the strong ethical restrictions severely limit their use for research

Significance of this study

How might it impact on clinical practice in the foreseeable future?

- ▶ The hBMSC-FRGS mice provide a novel platform for observing host-virus interactions and the progression of HBV-induced hepatitis and liver cirrhosis, which might be helpful for the development of novel antivirals and therapeutic strategies for HBV-related liver diseases.
- ▶ With further improvement and investigation, this liver and immune system dual-humanised mouse model might become useful for studying human immunity against HBV-related liver diseases.

purposes. Therefore, the development of an adequate liver and immune system dual humanised animal model that accurately delineates the natural history of HBV infection and immunopathophysiology is necessary for identifying strategies for early intervention and antiviral therapy. Four mouse models were recently developed through the co-transplantation of human fetal hepatocytes and syngeneic CD34⁺ haematopoietic stem cells (HSCs) or miss-matched human adult hepatocytes and HSCs, and these models were permissive to HBV or HCV infection and generated a mild immune response against the virus,^{7–10} but complete HBV or HCV disease progression to end-stage liver diseases has not been observed. Further translation is also critically limited by ethical issues and a shortage of available fetal donor hepatocytes with syngeneic HSCs.

As many studies have indicated, human bone marrow mesenchymal stem cells (hBMSCs) are easily isolated and differentiated into hepatocytes *in vitro* and *in vivo*.^{11–13} Our previous studies demonstrated that hBMSC transplantation rescued fulminant hepatic failure (FHF) in pigs and there were no immunological rejections occurred. The implanted hBMSCs efficiently proliferated and transdifferentiated into functional hepatocytes, and the recipient responses to liver damage were altered by immune regulation through paracrine effects.^{14–15} Other studies have also indicated that human mesenchymal stem cells are capable of differentiating into HSCs.^{16–19} These results imply that hBMSC-derived hepatocytes (hBMSC-Heps) in animals might be susceptible to HBV infection and that human immune responses against HBV might be activated by hBMSC-derived syngeneic immune cells.

In this study, we first set out to develop a liver and immune system dual humanised *Fah^{-/-} Rag2^{-/-} IL-2R γ ^{-/-} SCID* (FRGS) mouse model through hBMSC transplantation to delineate the natural course of HBV infection and disease progression (figure 1A, left). These animals, which we refer to as ‘hBMSC-FRGS’ mice, showed stable chimerism of hBMSC-Heps and syngeneic immune cell lineages and displayed a chronic HBV infection course similar to that observed in chronic HBV-infected (CHB) patients. Following HBV infection, we observed the full viral life cycle, including the production of HBV DNA, covalently closed circular DNA (cccDNA), surface antigen (HBsAg), e antigen (HBeAg), core antigen (HBcAg) and HBV-induced human immune and inflammatory responses and a subsequent progression to liver cirrhosis (figure 1A, right).

MATERIALS AND METHODS**Isolation, culture and identification of hBMSCs**

The hBMSCs were isolated through bone marrow (BM) aspiration from the iliac crest of healthy male volunteers. More details

regarding the methods used for hBMSC isolation, culture, phenotypic identification and multilineage differentiation are provided in online supplementary figure S1 and online supplementary materials and methods. Cells from passages 3 to 7 were used for the experiments.

Generation of hBMSC-FRGS mice through the transplantation of hBMSCs into FRGS mice with life-threatening FHF

Fah^{-/-} Rag2^{-/-} IL-2R γ ^{-/-} (FRG) mice were bred with BALB/c SCID mice to obtain FRGS mice. All the mice were bred in a specific pathogen-free (SPF) laboratory in the Animal Centre of Xiamen University. All the animal experiments were approved by the Ethics Committee of the State Key Laboratory of Molecular Vaccinology and Molecular Diagnostics and the National Institute of Diagnostics and Vaccine Development in Infectious Diseases of Xiamen University.

To enhance robust expansion of human-derived cells, life-threatening liver failure was induced by administration of the mouse hepatocyte-specific hepatotoxic hamster-anti-mouse CD95 antibody clone JO2 (JO2) and gradient 2-(2-nitro-4-fluoromethylbenzoyl)-1,3-cyclohexanedione (NTBC) withdrawal during the perioperative period.^{8–20} FRGS mice at 6–8 weeks of age were subjected to gradient NTBC withdrawal through their drinking water from day –14 to –8 and administered 100% NTBC from day 7 to 10 and an intraperitoneal JO2 injection (0.2 mg/kg) at days –1, 2, 5 and 8. To further eliminate murine immune cells and guarantee robust expansion of human immune cells, the mice received an intraperitoneal injection (25 mg/kg) of busulfan (dissolved in DMSO and diluted with 0.9% saline) at days –7, –3 and –1.⁸ For hBMSC transplantation, the FHF-FRGS mice received an intrasplenic injection of 1 × 10⁶ hBMSCs suspended in 0.4 mL of normal saline at day 0, and other FHF-FRGS mice received the same treatment without cell transplantation. The mice belonging to the normal FRGS group mice only received 100% NTBC in their drinking water (figure 1B). Animal surgery was performed under sterilised conditions and anaesthesia with isoflurane. To promote further expansion of hBMSC-Heps, the mice were cycled off NTBC every 2 weeks after 1 week following transplantation. To maintain the liver chimerism of hBMSC-Heps, the mice received persistent NTBC addition to their drinking water starting at week 10 after transplantation. Liver repair and regeneration by the transplanted hBMSCs were demonstrated by H&E staining of liver tissues and biochemical analyses of liver function-related markers.

Identification of the chimerism of hBMSC-Heps and hBMSC-derived immune cell lineages in hBMSC-FRGS mice

The chimerism of hBMSC-Heps was assessed by measuring the human albumin (hALB) levels in serum through a fluorescent-activated cell sorting (FACS) analysis of total liver cells isolated by collagenase perfusion. The isolated hBMSC-Heps and mouse livers were subjected to immunohistochemistry (IHC) and quantitative reverse transcription PCR (qRT-PCR) assays for the analysis of human hepatocyte-specific markers and genes. The serum hALB levels were measured by ELISA. The chimeric rates of hBMSC-Heps were evaluated by the linear relationship between the percentage of hALB⁺/human sodium-sodium taurocholate co-transporting polypeptide positive (hNTCP⁺) cells in perfused liver cells and the serum hALB levels. To identify the chimerism of hBMSC-derived immune cell lineages, BM, lymph node, peripheral blood, spleen and liver non-parenchymal cells were collected and analysed by FACS using human leucocyte markers as previously described.^{9–10, 21}

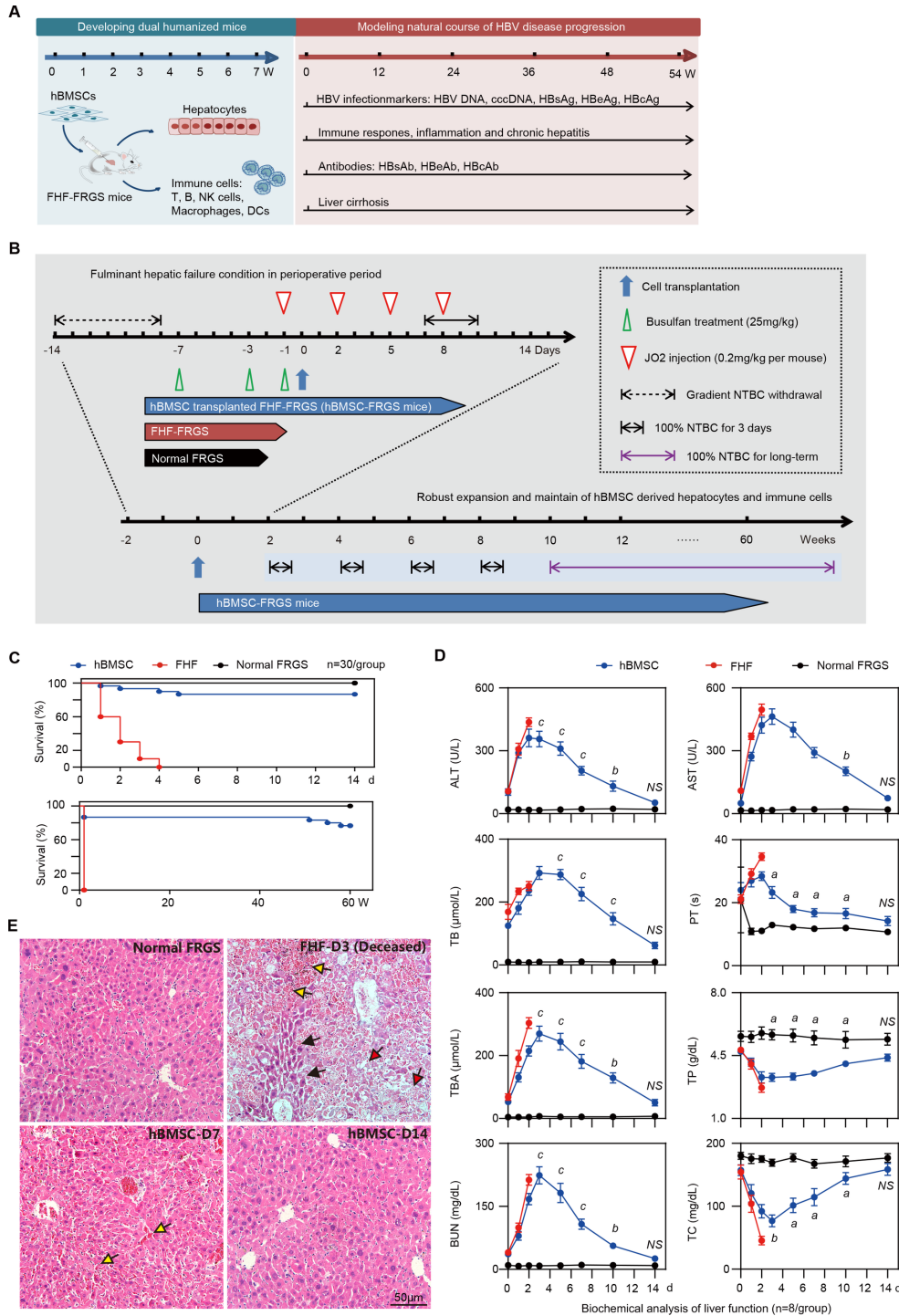


Figure 1 Generation of human bone marrow mesenchymal stem cells-*Fah*^{-/-} *Rag2*^{-/-} *IL-2Rγc*^{-/-} *SCID* (hBMSC-FRGS) mice through the transplantation of hBMSCs into fulminant hepatic failure (FHF)-FRGS mice. (A) Schematic design of the rescue of FRGS mice with life-threatening FHF by hBMSC transplantation, the generation of hBMSC-derived human hepatocytes and immune cell lineages, and the modelling of the progression of HBV infection-induced viremia, immune and inflammatory responses, antibody synthesis, chronic hepatitis and liver cirrhosis. (B) Schematic design of the cell transplantation treatments administered to mice. During the perioperative period, FHF-FRGS mice with or without hBMSC transplantation received the same treatments, including 2-(2-nitro-4-fluoromethylbenzoyl)-1,3-cyclohexanedione (NTBC) on-off treatment, JO2 and busulfan injection. FHF-FRGS mice with hBMSC transplantation received a splenic injection of 1×10^6 hBMSCs at day 0. The normal FRGS mice were administered 100% NTBC in their drinking water without any extra treatment. (C) Survival analysis of mice in the three groups during the perioperative period. The survival of hBMSC-FRGS and normal FRGS mice was observed for 60 weeks (n=30/group). (D) Temporal changes in eight typical biochemical markers of liver function (n=8/group). (E) H&E staining of liver tissue collected from FHF-FRGS with or without hBMSC transplantation and normal FRGS mice (bar=50 μm). The yellow arrow indicates the haemorrhage point, the red arrow indicates dead cells and the black arrow indicates residual cells. a) $P < 0.05$; b) $p < 0.01$; c) $p < 0.001$. ALT, alanine transaminase; AST, aspartate aminotransferase; BUN, blood urea nitrogen; cccDNA, covalently closed circular DNA; DC, dendritic cell; HBcAg, hepatitis B core antigen; HBeAg, hepatitis B e antigen; HBsAg, hepatitis B surface antigen; NS, not significant; PT, prothrombin time; TB, total bilirubin; TBA, total bile acid; TC, total cholesterol; TP, total protein.

The hBMSC-derived human immune cell lineages in liver tissues were identified by IHC and immunofluorescence (IF) staining. The functions of the hCD45⁺ cells isolated from the livers of hBMSC-FRGS mice were assessed by ELISAs of human cytokines after *in vitro* stimulation of phytohemagglutinin (PHA) and phorbol 12-myristate 13-acetate (PMA)/ionomycin. More details regarding the methods used for cell isolation, stimulation, FACS, ELISA, IHC, IF and qRT-PCR are provided in online supplementary figure S2 and in online supplementary materials and methods section.

Establishment and characterisation of HBV infection in hBMSC-FRGS mice

The four common HBV genotypes, namely, A, B, C and D, which have been recognised as highly epidemic HBV strains worldwide, were investigated. Because of its tendency to induce epidemics in Asia and its high pathogenicity, HBV genotype C is typically used for the long-term observation of HBV-induced liver diseases. The serum and intracellular HBV DNA levels were analysed using HBV X protein-specific probes and measured by qRT-PCR. The distributions of HBsAg⁺ and HBcAg⁺ cells were detected by IHC staining. The proportion of HBsAg⁺ cells in the population of hALB⁺ cells was analysed through cell counting of IHC results. The ratio of HBV DNA-positive cells in hALB⁺ cells was detected by fluorescence *in situ* hybridisation (FISH). The intracellular HBV cccDNA levels were measured by Southern blot and qRT-PCR. Details of the procedures used for HBV inoculation and virological measurements are provided in the online supplementary materials and methods section and in our previous publications.^{22,23}

Observations of immune and inflammatory responses, chronic hepatitis and liver cirrhosis

Liver cells of uninfected controls and HBV-infected hBMSC-FRGS mice were isolated by collagenase perfusion, and the cellularity of intrahepatic human immune cells was analysed by FACS. The levels of serum cytokines and HBV-specific antibodies were measured using corresponding ELISA kits. The expression of human cytokine-relevant genes in liver tissues was assessed by qRT-PCR. For observations of immune cell recruitment and chronic liver inflammation, paraffin and frozen sections of the indicated liver tissues were subjected to immunostaining and H&E staining.

The levels of the cirrhosis markers hyaluronic acid (HA) and gamma glutamate transpeptidase (GGT) in the mice serum were measured by ELISA. The expression of cirrhotic-relevant human genes in liver tissues was detected by qRT-PCR. For observations of pathological features and the progression of liver cirrhosis, paraffin sections collected from the indicated liver tissues were subjected to IHC and pathological staining analyses, which included H&E, Masson's trichrome (M&T), Van Gieson (VG) and sirius red/fast green (SR/FG) staining. Pathological analysis and progression of liver fibrosis to cirrhosis were diagnosed according to bulletin of WHO 'The morphology of cirrhosis: definition, nomenclature, and classification'^{24,25} by a pathologist with >10-year experience. Detailed criteria of liver fibrosis and cirrhosis are available in online supplementary materials and methods.

Statistics

The results of the measurements are presented as the means±SEMs. No statistical method was used to predetermine sample sizes. For comparisons between two groups, unpaired Welch's t-test was applied for calculating statistical probability in this study. For comparisons between more than two groups,

one-way analysis of variance followed by Tukey's post hoc test was applied. Statistical analysis was performed using Prism V.7 (GraphPad, La Jolla, California, USA).

More methodological details are provided in online supplementary materials and methods section and in online supplementary table 1 (reagents), table 2 (antibodies) and table 3 (primers).

RESULTS

hBMSC transplantation rescued FHF mice

The hBMSCs used in this study possessed typical mesenchymal stem cell phenotypes (positive for hCD90 and hCD29 but negative for hCD34 and hCD45) and multipotential differentiation characteristics (differentiate to adipocytes, osteocytes and hepatocyte-like cells *in vitro*), which were isolated from donor iliac crest (online supplementary figure S1). The FHF mouse model was induced by gradient withdrawal of NTBC and multiple injections of JO2 (for details, see figure 1B). The transplantation group mice received an intrasplenic injection of 1×10^6 hBMSCs, and the FHF-FRGS mice underwent a sham operation and received normal saline without cells. NTBC was added daily to the drinking water of normal FRGS mice (figure 1B). The analysis of survival during the perioperative period revealed that all the FHF-FRGS mice died within 4 days, and the implanted hBMSCs rescued 86.7% (26/30) of the mice from life-threatening FHF (figure 1C, top). The long-term survival observations revealed that 27 of 30 normal FRGS mice (90%) and 22 of 26 hBMSC-FRGS mice (84.6%) survived for >60 weeks (figure 1C, bottom). A biochemical analysis of eight representative liver and functional biomarkers, including alanine transaminase (ALT), aspartate aminotransferase (AST), total bilirubin (TB), total bile acid (TBA), total cholesterol (TC), blood urea nitrogen (BUN), total protein (TP) and prothrombin time (PT), showed that hBMSC transplantation significantly improved liver function (figure 1D). H&E staining further confirmed that the hBMSC transplantation was notably coupled with repair of the damaged liver structure at day 7, whereas the deceased FHF-FRGS mice showed the typical histology of a failed liver with extensive hepatic necrosis and haemorrhage at day 3 after transplantation (figure 1E). These results indicated that hBMSC transplantation rescued FHF-FRGS mice within the first week after the initial JO2 injection.

Chimerism of hBMSC-derived human hepatocytes in hBMSC-FRGS mice

Mouse serum, perfused liver cells and liver tissues were collected to investigate the chimerism of hBMSC-Heps. hALB was detectable in the mice serum at week 3, increased to 1.72 ± 0.07 mg/mL at week 12 and remained at 1.60 ± 0.13 mg/mL at week 60 after hBMSC transplantation (figure 2A). FACS showed that human leucocyte antigen (HLA)-positive cells were detectable in the entire population of mouse liver cells ($10.2\% \pm 0.7\%$) at week three, increased to $45.8\% \pm 1.5\%$ at week 12 and remained at $42.4\% \pm 1.0\%$ at week 60 after transplantation (figure 2B). Further analysis showed that $91.7\% \pm 1.0\%$, $90.2\% \pm 1.5\%$ and $1.8\% \pm 0.4\%$ of HLA⁺ cells were positive for hALB, HBV receptor hNTCP and hCD45, respectively, at week 12 after hBMSC transplantation, and these levels were maintained until week 60 (figure 2B). A correlation analysis between the percentages of hNTCP⁺ cells in the whole population of mouse liver cells with the serum hALB concentrations revealed that the average human hepatocyte chimerism reached $47.2\% \pm 2.5\%$ at week 12 after transplantation and that this level was maintained until week 60 after transplantation (figure 2C).

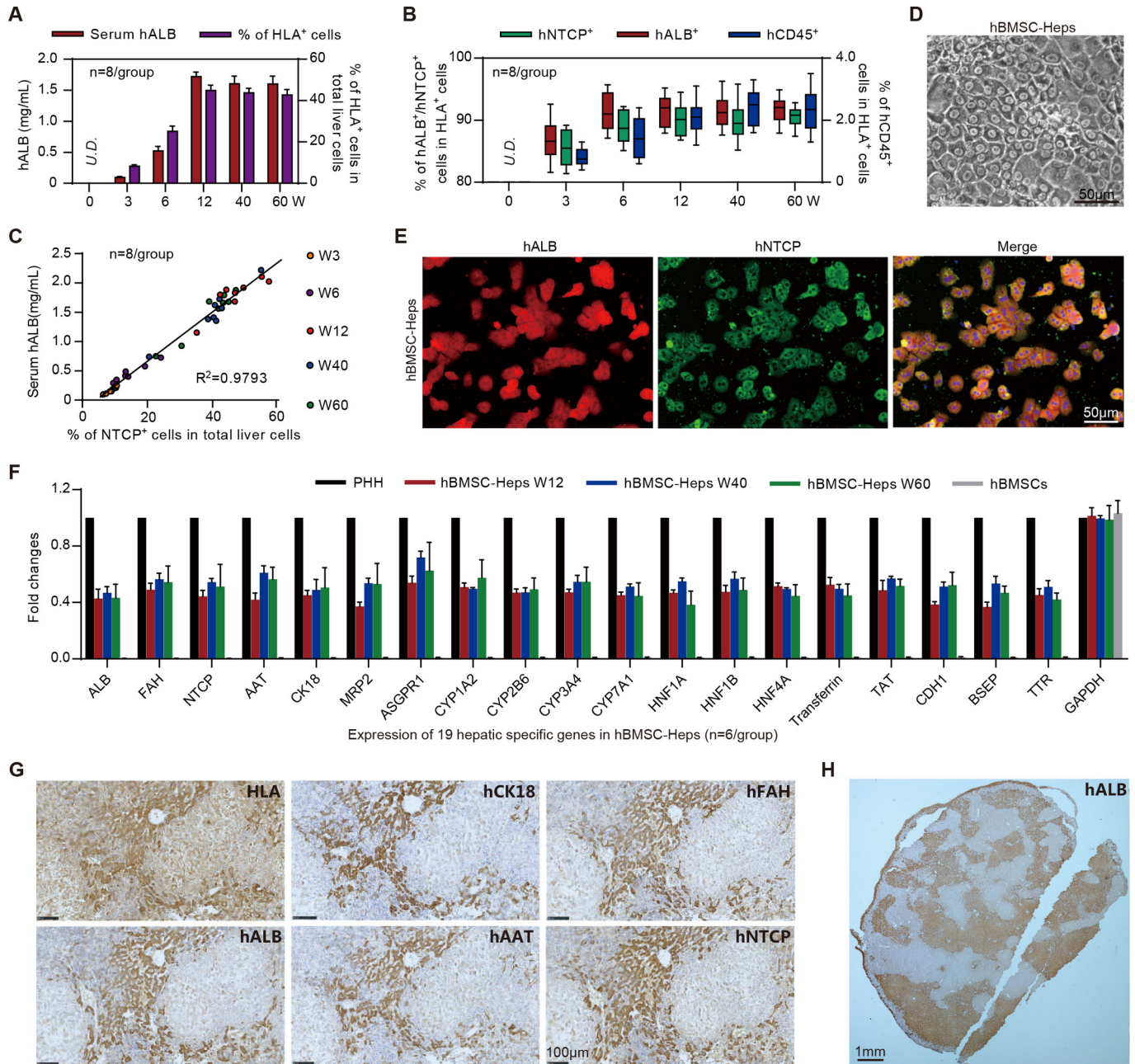


Figure 2 Characterisation of human bone marrow mesenchymal stem cell (hBMSC)-derived hepatocytes in hBMSC-*Fah*^{-/-} *Rag2*^{-/-} *IL-2Rγc*^{-/-} *SCID* (FRGS) mice. (A) Detection of the serum human albumin (hALB) level and percentage of human leucocyte antigen-positive (HLA⁺) cells in the total population of liver cells (n=8/group). (B) Percentage of hALB⁺, hNTCP⁺ and hCD45⁺ cells in the HLA⁺ cells from week 0 to 60 after hBMSC transplantation (n=8/group). (C) Correlation analysis between the serum hALB level and the percentage of hNTCP⁺ cells in the whole population of liver cells collected from hBMSC-FRGS mice (n=8/group). (D) Morphology of fluorescent-activated cell sorting (FACS)-sorted hALB⁺ hBMSC-hepatocytes (Heps) at week 12 after transplantation (bar=50 μm). (E) Detection of perfused hBMSC-Heps by immunofluorescence (IF) staining for hALB and hNTCP at week 12 after transplantation (bar=50 μm). (F) Quantitative reverse transcription PCR (qRT-PCR) analysis of the expression of 19 hepatic genes in the perfused hBMSC-Heps from week 12 to 60 after transplantation; primary human hepatocytes and hBMSCs were used as controls (n=6/group). (G) Immunohistochemistry (IHC) staining of liver tissues collected from hBMSC-FRGS mice at week 12 after transplantation for human hepatocyte markers, including hALB, hCK18, hAAT, hFAH and hNTCP (bar=100 μm). (H) IHC staining for hALB⁺ hBMSC-Heps in the whole liver lobe showed multiple distribution patterns, including periportal, non-periportal, scatter-like, island-like and cluster-like patterns (bar=1 mm). hFAH, human hepatocyte-specific fumarate dehydrogenase; hAAT, human hepatocyte-specific alpha-1-antitrypsin; hCK18, human hepatocyte-specific cytokeratin 18; hNTCP, human sodium-sodium taurocholate co-transporting polypeptide.

The phase-contrast microscopy image showed hALB⁺ hBMSC-Heps freshly isolated by FACS with a typical hepatocyte morphology in vitro (figure 2D). IF staining showed over 90% of hALB⁺ hBMSC-Heps were also positive for hNTCP (figure 2E). The qRT-PCR results showed that hALB⁺ hBMSC-Heps isolated

from hBMSC-FRGS mice stably expressed 19 human hepatocyte-specific genes from 12 to 60 weeks after transplantation (figure 2F). IHC staining of serial sections showed that the HLA⁺ cells were also positive for human hepatocyte-specific markers hALB, fumarate dehydrogenase (hFAH), alpha-1-antitrypsin

(hAAT), cytokeratin 18 (hCK18) and hNTCP (figure 2G). The whole liver lobe showed 58.7% chimerism of hALB⁺ cells and multiple distribution patterns (figure 2H). Additionally, no cell fusion between human-derived hepatocytes and mouse hepatocytes was observed in hBMSC-FRGS mice (online supplementary figure S3). Taken together, these results indicated the stable chimerism of hBMSC-Heps in hBMSC-FRGS mouse livers. A preliminary tumorigenicity assay revealed that, the surviving hBMSC-FRGS mice showed no evidence of tumours in the liver or other organs (including the brain, heart, lung, kidney, spleen, small gut and muscles) from week 0 to 60 after transplantation, as demonstrated by an analysis of human hepatocellular carcinoma specific markers in serum and liver tissue combined with H&E staining analysis (online supplementary figure S4). The above results indicated that hBMSC transplantation resulted in the generation of a humanised liver mouse model.

Chimerism of hBMSC-derived human immune cell lineages in hBMSC-FRGS mice

FACS results showed that the BM, thymus, lymph node, spleen, liver and peripheral blood of hBMSC-FRGS mice were reconstituted with varying amounts of hCD45⁺ cells at week 12 after transplantation (figure 3A, blue circle), whereas these cells were undetectable in the control FRGS mice (figure 3A, black circle). Further functional analysis of in vitro cultured hCD45⁺ cells enriched from the livers of hBMSC-FRGS mice had detectable levels of seven human-derived inflammatory cytokines (hTNF- α , hIFN- α , hIFN- γ , hIL-2, hIL-6, hIL-8 and hIL-10) 24 hours after stimulation with PHA and PMA/ionomycin (figure 3B). Unstimulated hCD45⁺ cells, which were used as controls, showed very low levels of these cytokines (figure 3B). An IHC analysis showed that human-derived immune cells (hCD45⁺), including human B cells (hCD19⁺), T cells (hCD4⁺ and hCD8⁺), natural killer (NK) cells (hNKp46⁺), macrophages (hCD86⁺ and hCD163⁺) and dendritic cells (hCD11c⁺ and hCD123⁺) were scattered in the liver tissue of hBMSC-FRGS mice at 12 weeks after transplantation (figure 3C).

Multiple human immune cell lineages derived from 10 different hBMSCs donors in the peripheral blood, spleen and liver of hBMSC-FRGS mice were subsequently assessed by FACS. The gating scheme and representative FACS plots of multiple human immune cell lineages in the livers of hBMSC-FRGS mice were displayed in figure 3D. The analysis of hBMSC-derived human immune cell lineages from 10 different donors (n=3/donor) at week 12 after transplantation revealed that hCD45⁺ cells constituted 34.5% \pm 3.3%, 30.6% \pm 2.7% and 45.2% \pm 2.9% of the total CD45⁺ (mCD45 and hCD45) cells in the peripheral blood, spleen and liver, respectively (figure 3E, line 1), and 27.0% \pm 2.4%, 29.5% \pm 2.6% and 33.6% \pm 2.3% of the total hCD45⁺ cells in the peripheral blood, spleen and liver, respectively, were hCD19⁺ B cells (figure 3E, line 2). In addition, hCD3⁺ T cells constituted 27.4% \pm 1.6%, 26.1% \pm 2.2% and 24.1% \pm 2.4% of the total population of hCD45⁺ cells in the peripheral blood, spleen and liver, respectively (figure 3E, line 3), and 4.1% \pm 0.3%, 4.2% \pm 0.3% and 3.9% \pm 0.4% of the total hCD45⁺ cells in the peripheral blood, spleen and liver, respectively, were hCD3⁺hNKp46⁺ NK cells (figure 3E, line 4). hCD3⁺hCD14⁺hCD68⁺ macrophages constituted 9.7% \pm 0.7%, 11.8% \pm 0.2% and 12.9% \pm 0.2% of the total hCD45⁺ cell population in the peripheral blood, spleen and liver, respectively (online supplementary figure S5A). Moreover, hCD3⁺hCD14⁺HLA-DR⁺dendritic cells (DCs) comprised 4.2% \pm 0.3%, 4.9% \pm 0.2% and 5.4% \pm 0.2% of the total hCD45⁺ cells in the

peripheral blood, spleen and liver, respectively (online supplementary figure S5B). These hBMSC-derived human immune cell lineages were maintained at comparable frequencies in the blood, spleen and liver until week 60 after transplantation (figure 3E and online supplementary figure S5).

Analysis of T cells revealed that the hCD3⁺ T cells in the spleen and liver exhibited a high hCD4/hCD8 ratio (with the majority of these cells being hCD4⁺ T cells) at both week 12 and 60 after transplantation (figure 3F). As demonstrated through an analysis of macrophages, 58.6% \pm 5.5% and 50.2% \pm 5.1% of the macrophage populations in the liver and spleen at week 12, respectively, were CD163⁺ M2 macrophages, 32.1% \pm 3.6% and 39.5% \pm 5.8% of these populations, respectively, were hCD86⁺ M1 macrophages, and these levels were maintained until week 60 after transplantation (figure 3G). An analysis of DCs showed that 71.1% \pm 4.9% and 74.2% \pm 3.2% of the DCs in the spleen and liver at week 12, respectively, were CD11c⁺ myeloid DCs, 18.2% \pm 4.4% and 19.9% \pm 1.8% of these populations, respectively, were hCD123⁺ plasmacytoid DC subset, and these levels were maintained until 60 after transplantation (figure 3H). These results demonstrated that a humanised immune cell mouse model with syngeneic human hepatocytes was developed.

hBMSC-FRGS mice support sustained HBV infection

To test the ability of hBMSC-Heps to support HBV infection, different single donor-derived hBMSC-FRGS mice exhibiting 40%–60% chimerism of human liver cells were infected with HBV genotype C. The serum hALB levels were maintained at 1.5–2.5 mg/mL throughout the infection course, and at 16 weeks post infection (w.p.i.), the HBV DNA, HBsAg and HBeAg levels were increased to 10⁷–10⁹ copies/mL (figure 4A), 10³–10⁴ IU/mL and 30–40 PEIU/mL (Paul Ehrlich Institute units), respectively (figure 4B). Serum HBV DNA and antigens were maintained at these high levels until 56 w.p.i. in HBV-infected hBMSC-FRGS mice (figure 4A and B) and were undetectable in the uninfected controls (online supplementary figure S6A and S6B).

To visualise the HBV distribution in the chimeric liver, liver tissues collected from the HBV-infected hBMSC-FRGS mice from 0 to 56 w.p.i. were subjected to IHC for the human liver protein hALB and HBV antigens. FRGS mice without transplantation and uninfected hBMSC-FRGS mice were used as controls. As shown by serial sections obtained from HBV-infected hBMSC-FRGS mice at 16 w.p.i., >80% of hALB-positive liver cells were co-positive for HBsAg and HBeAg (figure 4C), and the distribution and proportion of HBsAg-positive (HBsAg⁺) cells in hALB-positive (hALB⁺) liver cells varied over time. A statistical analysis of the IHC staining results from different fields of view showed that, the percentages of HBsAg⁺ cells in the population of hALB⁺ cells were 25.7% \pm 3.2% at 4 w.p.i., 54.1% \pm 5.1% at 8 w.p.i., 85.2% \pm 3.4% at 16 w.p.i., 78.1% \pm 4.4% at 32 w.p.i. and 73.4% \pm 5.2% at 56 w.p.i. (figure 4D). A FISH analysis showed that hBMSC-Heps isolated from HBV-infected hBMSC-FRGS mice were positive for HBV DNA at 4 w.p.i. (figure 4E). The quantitative results of a Southern blot analysis showed that intrahepatic HBV cccDNA was detectable in hBMSC-FRGS mice with chronic HBV infection (figure 4F and G). A regression analysis revealed a positive relationship among serum HBV DNA, serum HBsAg and intracellular HBV cccDNA (figure 4H). In addition, hBMSC-FRGS mice with comparable chimerism of human liver cells were also permissive for sustained infection with HBV genotypes A, B and D and showed similar trends in their serum HBV DNA, HBsAg and HBeAg levels (online supplementary figure S7). These

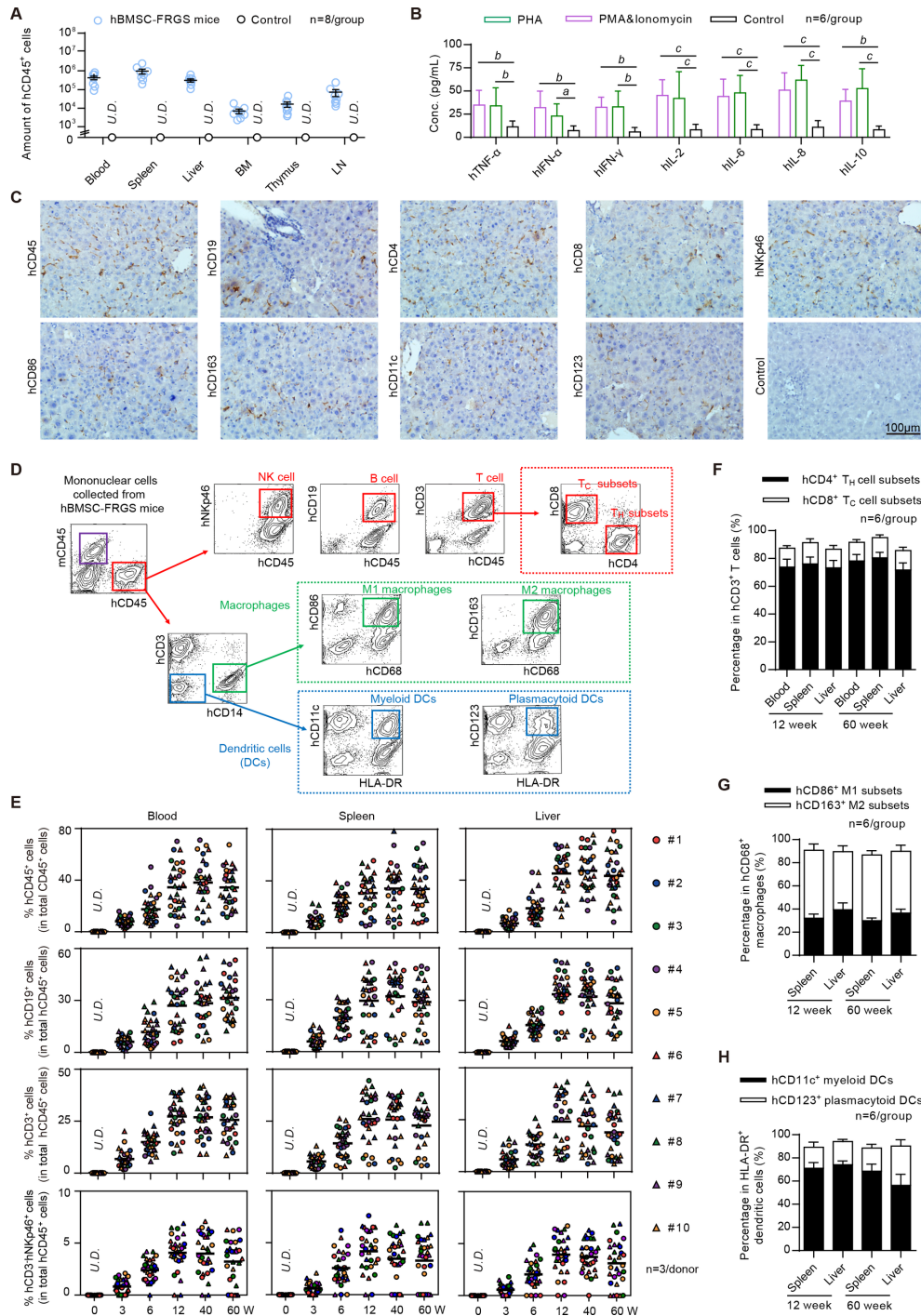


Figure 3 Characterisation of human bone marrow mesenchymal stem cell (hBMSC)-derived multiple immune cell lineages in hBMSC-*Fah*^{-/-} *Rag2*^{-/-} *IL-2RγC*^{-/-} *SCID* (FRGS) mice. (A) Total number of hCD45⁺ cells in the peripheral blood, spleen, liver, bone marrow (BM), thymus and lymph nodes in hBMSC-FRGS mice (blue circle) and control FRGS mice (black circle) at week 12 after transplantation (n=8/group). (B) Detection of human cytokine expression in hCD45⁺ cells isolated from the livers of hBMSC-FRGS mice and subjected to in vitro stimulation with phytohemagglutinin (PHA) (green column) or phorbol 12-myristate 13-acetate (PMA)/ionomycin (violet column) for 24 hours (n=6/group). hCD45⁺ cells without stimulation (black column) were used as controls. (C) Detection of hBMSC-derived human immune cells in the livers of hBMSC-FRGS mice at 12 weeks after transplantation by immunohistochemistry (IHC) for B cells (hCD19⁺), T cells (hCD4⁺ and hCD8⁺), natural killer (NK) cells (hNKp46⁺), macrophages (hCD86⁺ and hCD163⁺) and dendritic cells (DCs) (hCD11c⁺ and hCD123⁺) (bar=100 μm). (D) Gating scheme and representative fluorescent-activated cell sorting (FACS) contour plots of hBMSC-derived multiple human immune cell lineages in the livers of hBMSC-FRGS mice. (E) Reconstitution and maintenance of hCD45⁺ cells, hCD19⁺ B cells, hCD3⁺ T cells and hCD3⁺hNKp46⁺ NK cells in the peripheral blood, spleen and livers of hBMSC-FRGS mice from week 3 to 60 after transplantation (10 different donors, n=3). Relative proportions of (F) hCD4⁺ helper T (T_H) cells and hCD8⁺ cytotoxic T (T_C) cells within the population of hCD45⁺hCD3⁺ T cells in the spleen and liver of hBMSC-FRGS mice (n=6/group); (G) hCD86⁺ M1 and hCD163⁺ M2 subset within the population of hCD45⁺hCD3⁺hCD14⁺hCD68⁺ macrophages in the spleen and liver of hBMSC-FRGS mice (n=6/group) and (H) hCD11c⁺ myeloid and hCD123⁺ plasmacytoid subsets within the population of hCD45⁺hCD3⁺hCD14⁺HLA-DR⁺ DCs in the spleen and liver of hBMSC-FRGS mice (n=6/group). a) P<0.05; b) p<0.01; c) p<0.001. U.D., undetectable.

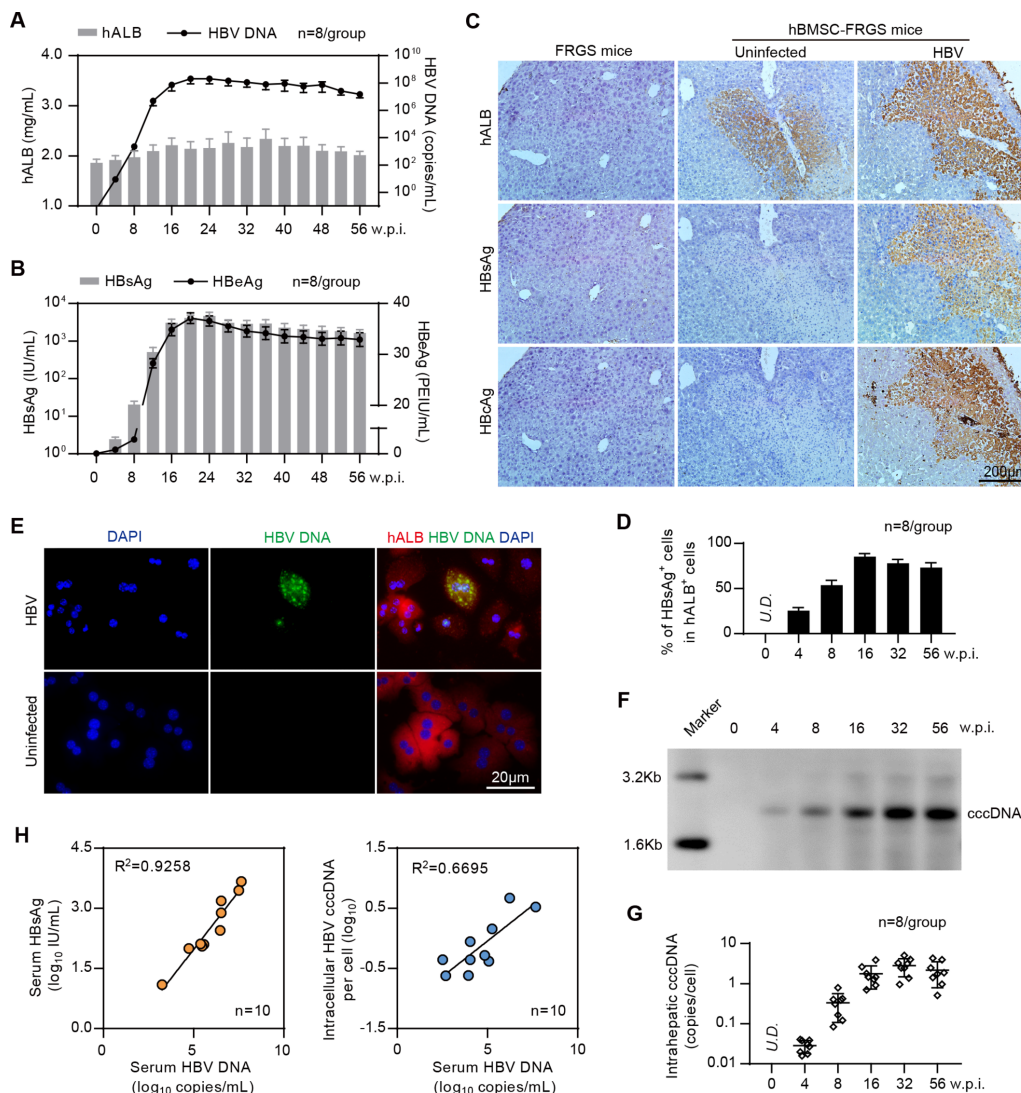


Figure 4 Establishment of sustained HBV infection in human bone marrow mesenchymal stem cell-*Fah*^{-/-} *Rag2*^{-/-} *IL-2R γ C*^{-/-} *SCID* (hBMSC-FRGS) mice. (A) Serum human albumin (hALB) (grey columns), HBV DNA (black lines), (B) hepatitis B surface antigen (HBsAg) (grey columns) and hepatitis B e antigen (HBeAg) (black lines) levels in hBMSC-FRGS mice inoculated with HBV (genotype C) from 0 to 56 weeks postinfection (w.p.i.) (n=8/group). (C) Immunohistochemistry (IHC) staining for hALB⁺, HBsAg⁺ and HBeAg⁺ cells of liver tissues collected from HBV-infected and uninfected hBMSC-FRGS mice and FRGS mice at 16 w.p.i. (bar=200 μm). (D) Statistical analysis of IHC images to determine the proportion of HBsAg⁺ cells in the population of hALB⁺ cells from 0 to 56 w.p.i. (n=8/group). (E) Fluorescence in situ hybridisation (FISH) analysis for HBV DNA in the population of hALB⁺ cells collected from HBV-infected hBMSC-FRGS mice and uninfected controls at 4 w.p.i. (bar=20 μm). Detection of intrahepatic HBV covalently closed circular DNA (cccDNA) levels in HBV-infected hBMSC-FRGS mice from 0 to 56 w.p.i. by (F) Southern blot and (G) quantitative reverse transcription PCR (qRT-PCR) (n=8/group). (H) Analysis of the correlation between the serum HBV DNA and serum HBsAg levels and the correlation between the serum HBV DNA and intracellular HBV cccDNA levels (n=10). PEIU, Paul Ehrlich Institute units.

results demonstrated the establishment of sustained HBV infection in hBMSC-FRGS mice.

Human-derived immune and inflammation responses and chronic hepatitis developed spontaneously after HBV infection in hBMSC-FRGS mice

To assess the cellular immune responses against HBV infection in hBMSC-FRGS mice, liver cells were perfused from 0 to 48 w.p.i. and analysed by FACS. The amount of intrahepatic hCD45⁺ cells significantly increased following HBV infection (figure 5A, top left). HBV-infected hBMSC-FRGS mice exhibited a 3.2-fold increase in intrahepatic hCD45⁺hCD3⁺hNKp46⁺ NK cell frequencies at 12 w.p.i., and these levels were reduced to the normal levels at 24 w.p.i. (figure 5A, top right). The frequencies

of intrahepatic hCD45⁺hCD3⁺hCD68⁺ macrophages and hCD45⁺hCD3⁺ T cells showed gradual increases to levels that were 4.4-fold and 2.5-fold higher than the baseline levels at 24 w.p.i., respectively, and these increased levels were maintained until 48 w.p.i. (figure 5A, bottom). Furthermore, IF of the livers from HBV-infected hBMSC-FRGS mice revealed abundant hCD68⁺ macrophages throughout the liver parenchyma and intertwined between HBsAg⁺ hepatocytes (figure 5B).

The presence of human-derived cytokines, which are important mediators in liver immunopathological injury during sustained HBV infection, in hBMSC-FRGS mice was detected by ELISA, and the results showed a persistent release of four types of cytokines into serum from 2 to 48 w.p.i. In contrast to the uninfected controls, the HBV-infected mice had significantly increased

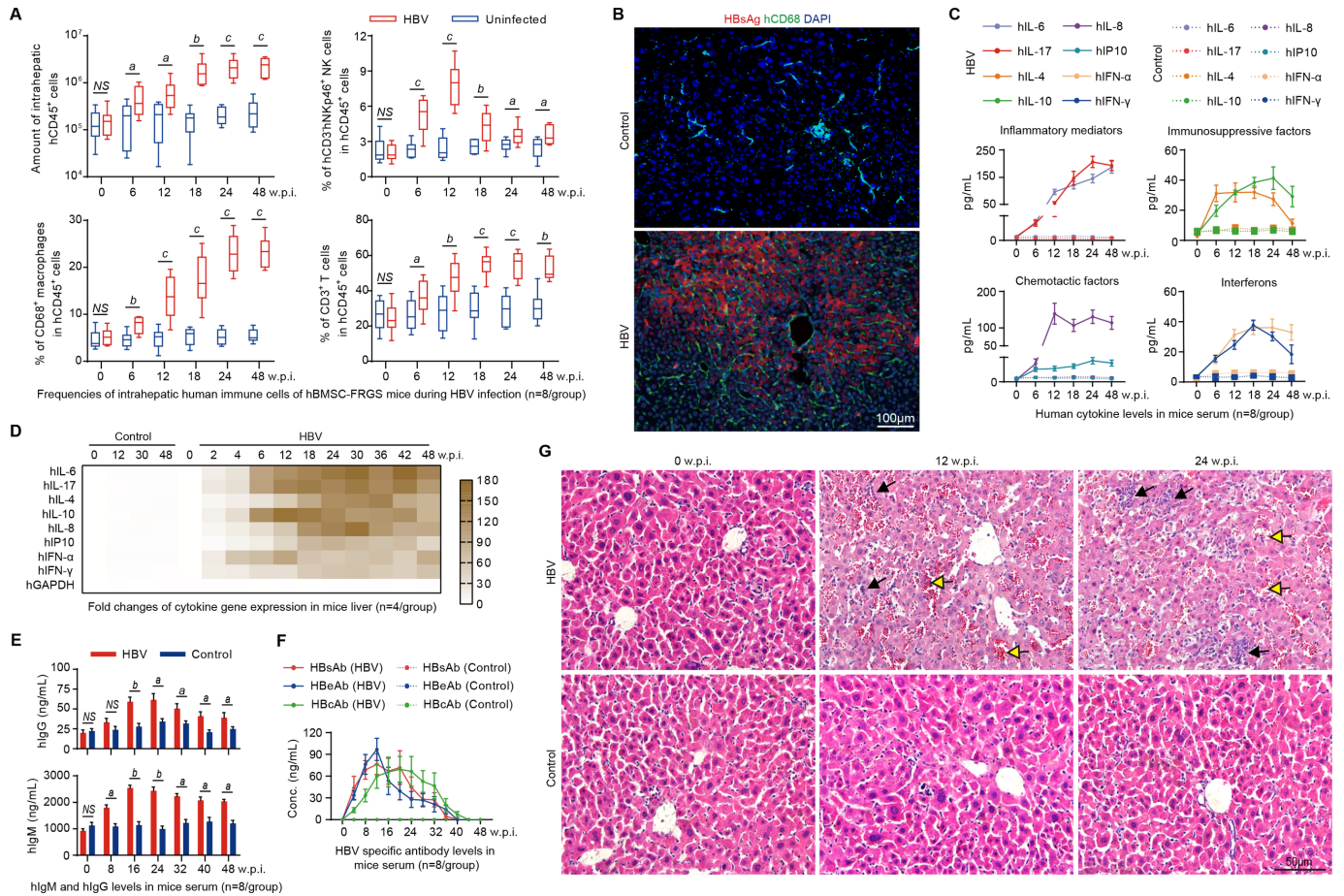


Figure 5 Chronic HBV infection induced immune and inflammatory responses and chronic hepatitis in the human bone marrow mesenchymal stem cell-*Fah*^{-/-} *Rag2*^{-/-} *IL-2Rγ*^{c/-} *SCID* (hBMSC-FRGS) mice. (A) Amount of hCD45⁺ cells (top left) and percentages of hCD45⁺hCD3⁺hNKp46⁺ natural killer (NK) cells (top right), hCD45⁺hCD3⁺hCD68⁺ macrophages (bottom left) and hCD45⁺hCD3⁺ T cells (bottom right) in the livers of uninfected controls and HBV-infected hBMSC-FRGS mice from 0 to 48 weeks postinfection (w.p.i.) (n=8/group). (B) Liver sections from uninfected controls (top) and HBV-infected hBMSC-FRGS mice (bottom) at 24 w.p.i. were co-stained for hepatitis B surface antigen (HBsAg) (red) and hCD68 (green). 4',6-diamidino-2-phenylindole (DAPI)-stained nuclei are shown in blue (bar=100 μm). (C) Plasma sample from uninfected controls and HBV-infected hBMSC-FRGS mice were analysed by ELISA for various human cytokines (n=8/group). (D) Quantitative reverse transcription PCR (qRT-PCR) analysis for the expression of human cytokine genes in HLA⁺ liver cells collected from uninfected controls and HBV-infected hBMSC-FRGS mice (n=4/group). (E) ELISA for the concentrations of hIgM and hIgG in sera of uninfected controls and HBV-infected hBMSC-FRGS mice (n=8/group). (F) ELISA for the concentrations of HBsAg antibody (HBsAb), HBeAg antibody (HBeAb) and HBcAg antibody (HBcAb) in sera of uninfected controls and HBV-infected hBMSC-FRGS mice (n=8/group). (G) H&E staining of liver tissues collected from uninfected controls and HBV-infected hBMSC-FRGS mice. The yellow arrow indicates the haemorrhage point, and the black arrow indicates the recruitment and infiltration of immune cells (bar=50 μm). a P<0.05; b p<0.01; c p<0.001). NS, not significant.

levels of the inflammatory mediators' hIL-6 and hIL-17 and of the immunosuppressive factors hIL-4 and hIL-10 from 2 to 48 w.p.i. (figure 5C). The levels of the chemotactic factors hIL-8 and hCXCL10, as well as hIFN-α and hIFN-γ, were increased from 2 to 24 w.p.i., and this trend was maintained throughout the same course of infection (figure 5C). The immunosuppressive factors hIL-23, hIL-27, hIL-2, hIL-32 and hTNF-α, the immunosuppressive factors hIL-1ra and hIL-13, chemotactic factor hCXCL9 and hIFN-β also showed a similar slight increase during the same infection course (online supplementary figure S8A). qRT-PCR results further confirmed similar trends for these human inflammatory-related cytokine genes in liver tissues collected from HBV-infected hBMSC-FRGS mice during the same infection course (figure 5D and online supplementary figure S9B). HBV-infected mice showed a significant increase in the human-derived IgM serum levels and a mild increment in the hIgG levels (figure 5E). ELISAs for HBV antibodies revealed that

the serum concentrations of HBsAg antibody (HBsAb), HBeAg antibody (HBeAb) and HBcAg antibody (HBcAb) increased to 53.6±18.9 ng/mL, 146.2±15.4 ng/mL and 46.2±15.4 ng/mL at 12 to 16 w.p.i., respectively, and these levels were maintained until week 32 w.p.i. and then gradually decreased (figure 5F). The serological changes in hIgM, hIgG, HBsAb, HBeAb and HBcAb in individual animals were presented in online supplementary figure S8C,D. Furthermore, the majority of HBsAb and HBcAb were IgM, rather than IgG at 24 w.p.i. (online supplementary figure S8E).

Observations of the pathological changes in the liver during the HBV infection course, as demonstrated though H&E staining, showed an acute hepatitis pattern with significant lobular inflammation, lymphoid aggregates and duct lesions at 12 w.p.i. Chronic hepatitis patterns with varying degrees of predominantly lymphocytic portal inflammation and interface hepatitis were observed in hBMSC-FRGS mice at 24 w.p.i., whereas

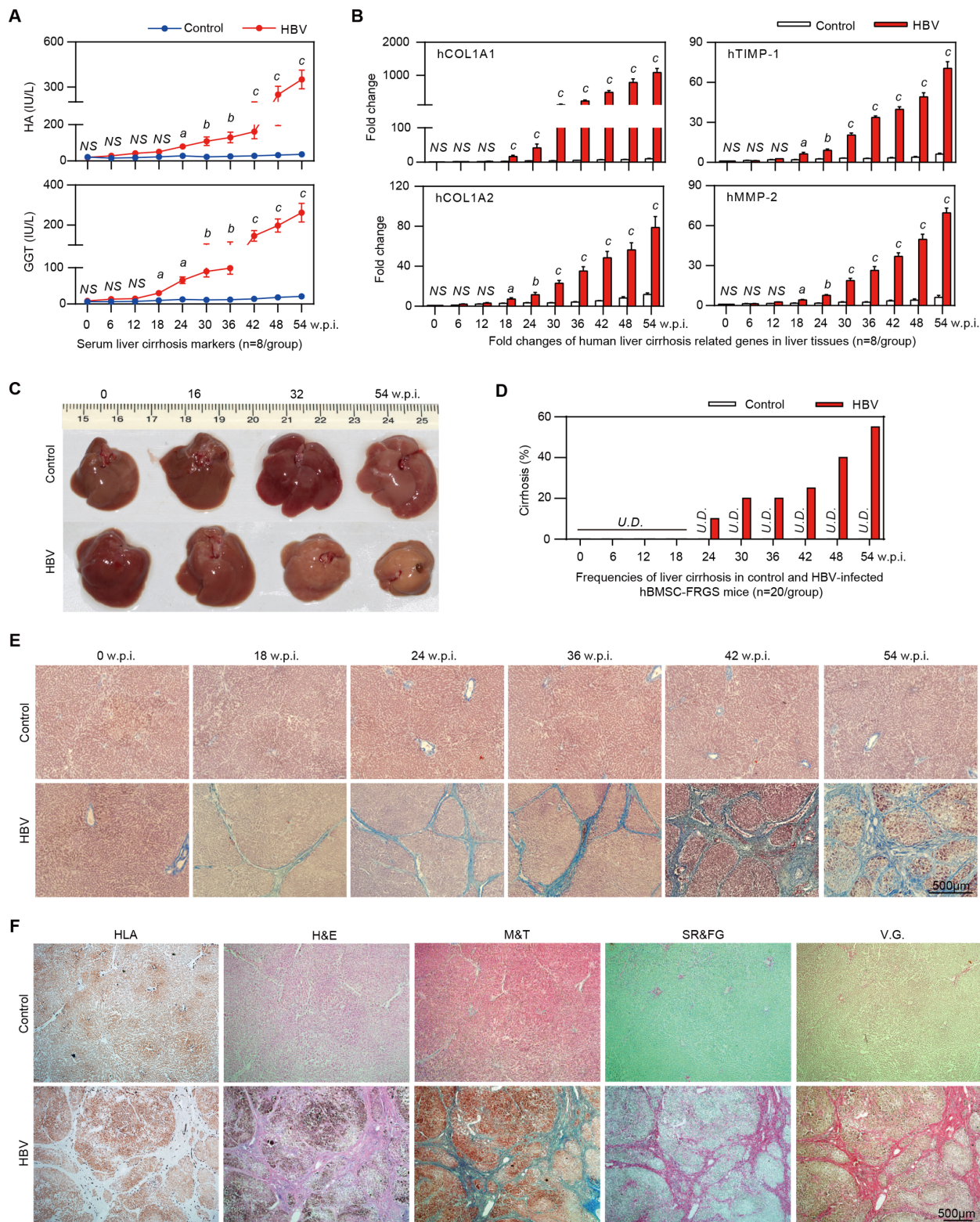


Figure 6 Progression of chronic HBV infection induced liver cirrhosis. (A) Concentration of the liver cirrhosis markers hyaluronic acid (HA) and gamma glutamate transpeptidase (GGT) in serum of uninfected controls (blue line) and HBV-infected human bone marrow mesenchymal stem cell-*Fah^{-/-} Rag2^{-/-} IL-2R γ C^{-/-} SCID* (hBMSC-FRGS) mice (red line) (n=8/group). (B) quantitative reverse transcription PCR (qRT-PCR) analysis of the expression of four human cirrhosis-related genes in liver tissues collected from uninfected controls (white column) and HBV-infected hBMSC-FRGS mice (red column) (n=8/group). (C) Morphology of liver cirrhosis and (D) statistical analysis of related morbidity in uninfected controls (white column) and HBV-infected hBMSC-FRGS mice (red column) during a 54-week HBV infection course (n=20/group). (E) M&T staining of liver tissues collected from uninfected controls and HBV-infected hBMSC-FRGS mice during the progression of HBV-induced liver cirrhosis (bar=500 µm). (F) Immunohistochemistry (IHC) staining for human leucocyte antigen (HLA) and pathological staining (H&E, M&T, SR/FG and VG) of serial sections collected from uninfected controls and HBV-infected hBMSC-FRGS mice with typical liver cirrhosis (bar=500 µm). a) P<0.05; b) p<0.01; c) p<0.001. NS, not significant; U.D., undetectable; w.p.i., weeks postinfection.

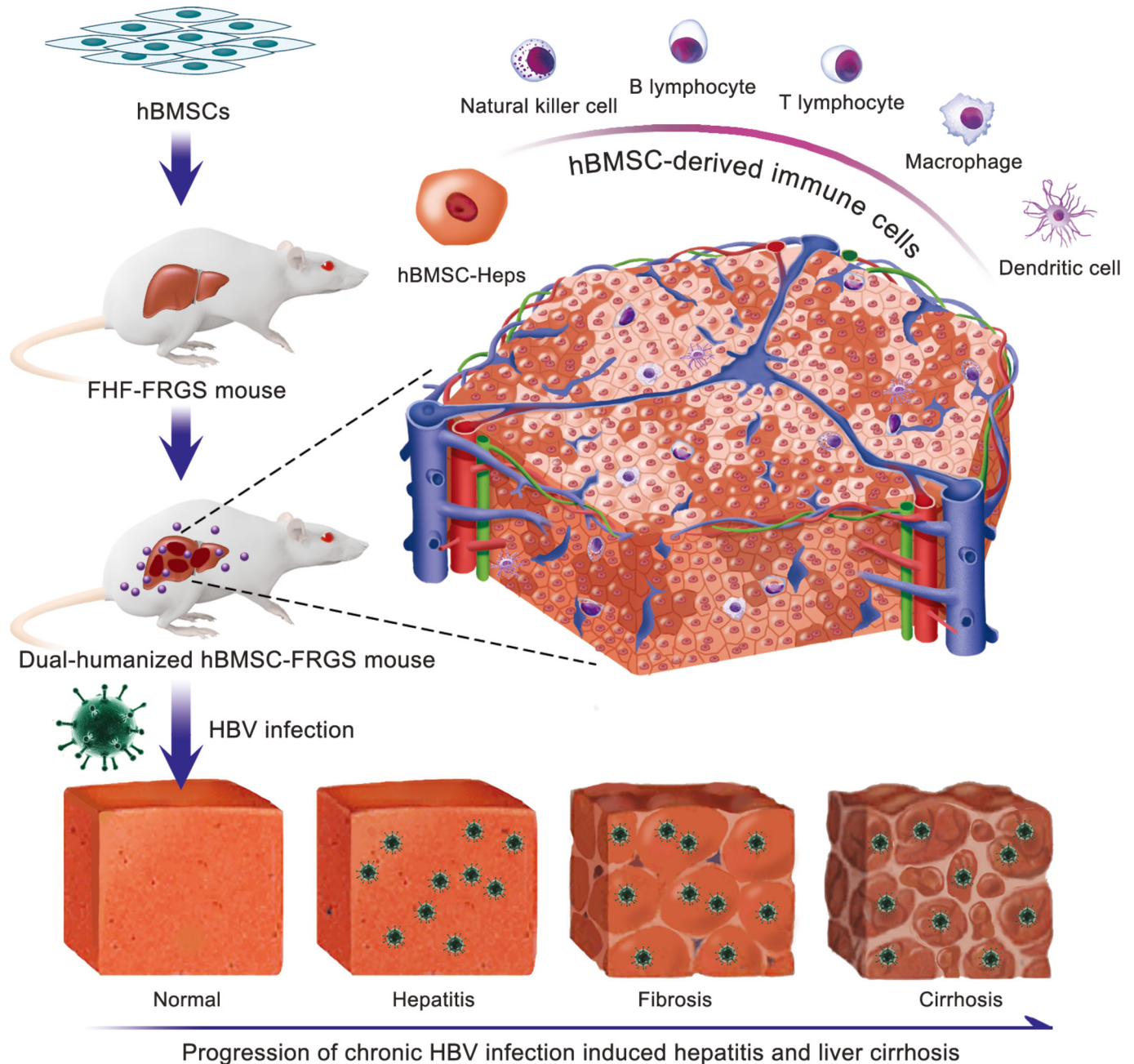


Figure 7 Progression of chronic HBV infection induced hepatitis and liver cirrhosis in dual humanised human bone marrow mesenchymal stem cell-*Fah^{-/-} Rag2^{-/-} IL-2R γ c^{-/-} SCID* (hBMSC-FRGS) mice. A novel dual-humanised mouse model with efficient chimerism of human liver cells and human immune cell lineages was developed using a single transplantation of hBMSCs, which were sensitive to chronic HBV infection and generated sustained human immune and inflammatory responses that led to liver cirrhosis. FHF, fulminant hepatic failure.

the liver tissues collected from uninfected hBMSC-FRGS mice showed no pathological changes during this period (figure 5G). Furthermore, eight representative liver functional biomarkers in the serum revealed liver injury in HBV-infected hBMSC-FRGS mice (online supplementary figure S8F). These results showed that hBMSC-FRGS mice displayed the typical immunopathology characteristics observed during the course of chronic HBV infection, which indicated that these mice exhibited a chronic hepatitis pattern similar to the one observed in CHB patients.

Progression of liver cirrhosis in HBV-infected hBMSC-FRGS mice

Serological and histological analyses were performed to determine HBV-induced liver cirrhosis in hBMSC-FRGS mice. The

detection of serological cirrhotic markers showed that the HA and GGT levels were significantly increased from 18 to 54 w.p.i. (figure 6A, red line), and qRT-PCR indicated that four human fibrosis-relevant genes (hCOL1A1, hCOL1A2, hTIMP-1 and hMMP-2) were significantly and simultaneously elevated (figure 6B, red column).

Preliminary observations revealed that the gross appearance of a normal liver is reddish brown in colour and has a soft consistency and smooth surface, whereas the cirrhotic liver collected from HBV-infected hBMSC-FRGS mice from 0 to 54 w.p.i. exhibited the typical morphology of cirrhosis, with diffused scars, nodules and a subsidence area (figure 6C). Liver tissues from uninfected controls and HBV-infected hBMSC-FRGS mice were collected from 0 to 54 w.p.i. for M&T staining. According

to globally accepted criteria,^{24 25} liver cirrhosis was observed in 10% (2/20) of the HBV-infected hBMSC-FRGS mice at 24 w.p.i. and in 55% (11/20) of the mice at 54 w.p.i. (figure 6D, red column). In contrast, no pathological features of liver cirrhosis were observed in the uninfected controls (figure 6D, white column). The M&T staining results showed that, the progression of liver fibrosis to cirrhosis from 24 to 54 w.p.i. exhibited the typical characteristics, including increased collagenous accumulation, fibre hyperplasia, an abnormal hepatic lobule structure, platelet collapse and nodule formation (figure 6E and online supplementary figure S9). IHC staining showed that the cirrhotic nodules were positive for HLA. Confluent necrosis with residual inflammation and scarring varying from mild portal expansion to periportal fibrous strands and bridging fibrosis with loss of architecture and nodule formation were observed during this period (figure 6F). These results demonstrated that the progression and characteristics of chronic HBV infection-induced liver cirrhosis in hBMSC-FRGS mice were similar to the disease pattern observed in CHB patients.

DISCUSSION

A number of chemical-based, diet-based and surgery-based as well as genetically modified cirrhosis models have been commonly used to elucidate the mechanisms involved in end-stage liver cirrhosis.²⁶ However, due to the difficulties associated with reconstructing the human immune system in animals, few infection-based animal models have been developed to reflect the natural progression of HBV-induced cirrhosis.²⁷

As we and other researchers have reported, hBMSCs have many benefits, including immune tolerance, easy procurement and potential transdifferentiation into multiple lineages,^{14 15 28} and the development of dual humanised mouse models through a single transplantation of hBMSCs might overcome the above-mentioned limitations.^{29 30} In a recent study, the A2/NSG-hu HSC/Hep mouse model generated with JO2 administration showed significantly higher serum hALB levels and amounts of hCD45⁺ cells in blood than the model without JO2 administration,⁸ suggesting that JO2-induced FHF is essential to establish high chimerism of both hBMSC-derived hepatocytes and immune cells. Compared with mild liver injury, which was used in previous studies, FHF was used in this study because it provides more adequate space and conditions for supporting hBMSC proliferation and transdifferentiation into human hepatocytes and multiple immune cell lineages, including myeloid and lymphoid cells (B cells, T cells, NK cells, macrophages and DCs), and as a result, the use of this model generated significant chimerism of both human hepatocytes and syngeneic immune cells in the liver, spleen, peripheral blood, BM, thymus and mesenteric lymph nodes. Our previous study and others have demonstrated that hBMSCs can secrete many useful cytokines, including IL-3, granulocyte-macrophage colony-stimulating factor (GM-CSF) and granulocyte colony-stimulating factor (G-CSF), through paracrine effects,^{15 31} and these cytokines might be helpful for improving the development and maturation of human immune cell lineages. Our model system involving FHF conditions and a single transplantation of hBMSCs showed that HBV infection-based animal models exhibited human immunity could be produced with high reproducibility. Clarifying the detailed chimerism mechanisms associated with the cell transdifferentiation or fusion of implanted stem cell into human hepatocytes and multiple lineages of human immune cells *in vivo* will be an interesting research direction.³²⁻³⁴

Recently, several mouse models, such as A2/NSG-hu HSC/Hep, HIS-Hep FRGN and HIS-HUHEP mouse, have been demonstrated as promising alternatives for HBV infection and chronic liver injury through co-transplantation with human fetal or primary hepatocyte and syngeneic HSCs.⁸⁻¹⁰ However, the permanent human immune responses and further development of cirrhosis need to be improved. Moreover, an animal model with HBV infection-based cirrhosis has not yet been developed. Similar to the findings obtained in our previous large animal studies in pigs,^{14 15} in this study, the implanted hBMSCs rescued mice from life-threatening FHF, repaired the damaged liver structure and ensured long-term survival for over 60 weeks with significant and persistent dual chimerism of human hepatocytes and multiple immune cell lineages. Based on this efficient dual chimerism, an almost life-long (56 weeks) chronic HBV infection course was established in the generated hBMSC-FRGS mice. A serological analysis of HBV antigens and antibodies demonstrated sustained viremia and immune response against HBV infection. Biochemical and cytokine evaluations revealed continuing deterioration of liver function and persistent increases in the levels of many inflammatory cytokines, which indicated chronic and severe progression of HBV infection in the recipient animals. Serological tests and IHC also demonstrated that HBV-induced liver cirrhosis spontaneously developed in the hBMSC-FRGS mice, with a 55% occurrence after 54 weeks of persistent HBV infection. The hBMSC-FRGS mice generated in this study constitute a system to display broad and robust virus-host interactions and immunopathophysiology during chronic hepatitis and liver cirrhosis progression, including cellular immune responses, cytokine levels, expression of disease-related genes and biochemical and pathological changes in the liver.

Clinically, immune and inflammation mechanisms are very complicated and primarily contribute to the progression and outcome of HBV infection.^{35 36} Our HBV-infected hBMSC-FRGS mice showed continuous progression to chronic liver diseases, similar to the pattern observed in CHB patients, and this progression was particularly noticeable for chronic hepatitis and liver cirrhosis, which might depend on sustained immune attacks, inflammatory reactions and incomplete repair. However, our hBMSC-FRGS mice also have some limitations, including an unclear mechanism regarding the origin of human immune cells and lower HBV antigen-specific antibody levels during the course of HBV infection. The immunopathogenesis of the recipient's response to HBV infection, including human leucocyte chemotaxis, hepatocyte damage and chronic HBV or severe progression, also needs to be clarified. Many factors, including cellular permissiveness to HBV, general immune-mediated suppression, HBV antigen-specific T-cell responses and antibody levels, might impact the clearance of HBV infection.³⁷ The decrease in the levels of HBV antigen-specific antibodies observed with sustained viremia in our system might be induced by immune tolerance, including increased amounts and proportions of hFoxp3⁺hCD4⁺ regulator T cells (Tregs) and hPD-1⁺hCD8⁺ exhausted T_c cells.^{10 38} Moreover, the role of each human cell subset and their interactions in the initiation of liver fibrosis and progression to cirrhosis are very complex and remain unclear in both CHB patients and animal models with chronic HBV infection.^{26 39} Therefore, our new model combined with the recently developed mass cytometry technique^{40 41} provides a new platform for investigating these unknown and complex mechanisms. Further improvements to this dual humanised system of immunocompetent animals for HBV, HCV and other hepatotropic viruses will also lead to exciting research discoveries.

In summary, we developed a novel dual humanised mouse model with efficient chimerism of human liver cells and human immune cell lineages using a single transplantation of hBMSCs, which were sensitive to chronic HBV infection and generated sustained human immune and inflammatory responses that led to liver cirrhosis (figure 7). Our system, which is easily reproduced, constitutes a new animal model that successfully recapitulates the natural disease progression of HBV infection and thus opens opportunities for understanding viral immune pathophysiology and improving the intervention strategies for HBV-related liver diseases.

Author affiliations

¹State Key Laboratory of Molecular Vaccinology and Molecular Diagnostics, National Institute of Diagnostics and Vaccine Development in Infectious Diseases, School of Life Sciences and School of Public Health, Xiamen University, Xiamen, China

²State Key Laboratory for Diagnosis and Treatment of Infectious Diseases, Collaborative Innovation Center for Diagnosis and Treatment of Infectious Diseases, The First Affiliated Hospital, Zhejiang University School of Medicine, Hangzhou, China

³Department of Pathology, The First Affiliated Hospital, Zhejiang University School of Medicine, Hangzhou, China

⁴Department of Microbiology and Molecular Genetics, New Jersey Medical School, Rutgers University, Newark, New Jersey, USA

Contributors

LY, JJ and XL contributed equally to this work. LY, JJ, XL, LZ, JJ, DS, YZ and SS established the cell culture system and performed the measurements of hBMSCs. LY, LX, LZ, YZ, TW and KW generated the animal model. LY, XL, JC and XG performed the HBV infection studies. LY, JJ, XL, LZ and JL (the 12th author) performed the histological analyses of chronic hepatitis and liver cirrhosis. WH, TZ, HZ, JZ and QY participated in the experimental design and data analyses. JL (the 22th author), LZ, JJ and XL wrote the manuscript. TC, JL (the 22th author) and NX supervised the project.

Funding This work was supported by the National Science and Technology Major Project (grant nos. 2017ZX10304402, 2017ZX10203201 and 2018ZX09711003-005-003), the National Natural Science Foundation of China (grant nos. 81672023, 81571818 and 81771996), the Scientific Research Foundation of the State Key Laboratory of Molecular Vaccinology and Molecular Diagnostics (grant no 2016ZY005), Zhejiang Province and State's Key Project of the Research and Development Plan of China (grant nos 2017C01026 and 2016YFC1101304/3).

Competing interests None declared.

Patient consent Obtained.

Provenance and peer review Not commissioned; externally peer reviewed.

Open access This is an open access article distributed in accordance with the Creative Commons Attribution Non Commercial (CC BY-NC 4.0) license, which permits others to distribute, remix, adapt, build upon this work non-commercially, and license their derivative works on different terms, provided the original work is properly cited, appropriate credit is given, any changes made indicated, and the use is non-commercial. See: <http://creativecommons.org/licenses/by-nc/4.0/>.

REFERENCES

- Trépo C, Chan HL, Lok A. Hepatitis B virus infection. *Lancet* 2014;384:2053–63.
- Dienstag JL. Hepatitis B virus infection. *N Engl J Med* 2008;359:1486–500.
- Allweiss L, Dandri M. Experimental in vitro and in vivo models for the study of human hepatitis B virus infection. *J Hepatol* 2016;64:S17–31.
- de Jong YP, Rice CM, Ploss A. New horizons for studying human hepatotropic infections. *J Clin Invest* 2010;120:650–3.
- Dandri M, Petersen J. Chimeric mouse model of hepatitis B virus infection. *J Hepatol* 2012;56:493–5.
- Thomas E, Liang TJ. Experimental models of hepatitis B and C - new insights and progress. *Nat Rev Gastroenterol Hepatol* 2016;13:362–74.
- Washburn ML, Bility MT, Zhang L, et al. A humanized mouse model to study hepatitis C virus infection, immune response, and liver disease. *Gastroenterology* 2011;140:1334–44.
- Bility MT, Cheng L, Zhang Z, et al. Hepatitis B virus infection and immunopathogenesis in a humanized mouse model: induction of human-specific liver fibrosis and M2-like macrophages. *PLoS Pathog* 2014;10:e1004032.
- Billerbeck E, Mommersteeg MC, Shlomai A, et al. Humanized mice efficiently engrafted with fetal hepatoblasts and syngeneic immune cells develop human monocytes and NK cells. *J Hepatol* 2016;65:334–43.
- Dusséaux M, Masse-Ranson G, Darche S, et al. Viral load affects the immune response to hbv in mice with humanized immune system and liver. *Gastroenterology* 2017;153:1647–61.
- Lee KD, Kuo TK, Whang-Peng J, et al. In vitro hepatic differentiation of human mesenchymal stem cells. *Hepatology* 2004;40:1275–84.
- Peng L, Xie DY, Lin BL, et al. Autologous bone marrow mesenchymal stem cell transplantation in liver failure patients caused by hepatitis B: short-term and long-term outcomes. *Hepatology* 2011;54:820–8.
- Lin BL, Chen JF, Qiu WH, et al. Allogeneic bone marrow-derived mesenchymal stromal cells for hepatitis b virus-related acute-on-chronic liver failure: a randomized controlled trial. *Hepatology* 2017;66:209–19.
- Li J, Zhang L, Xin J, et al. Immediate intraportal transplantation of human bone marrow mesenchymal stem cells prevents death from fulminant hepatic failure in pigs. *Hepatology* 2012;56:1044–52.
- Shi D, Zhang J, Zhou Q, et al. Quantitative evaluation of human bone mesenchymal stem cells rescuing fulminant hepatic failure in pigs. *Gut* 2017;66:955–64.
- Włodarski KH. Haematopoietic and osteogenic bone marrow stem cells. *Ortop Traumatol Rehabil* 2011;13:439–47.
- Freisinger E, Cramer C, Xia X, et al. Characterization of hematopoietic potential of mesenchymal stem cells. *J Cell Physiol* 2010;225:888–97.
- Cheng L, Qasba P, Vanguri P, et al. Human mesenchymal stem cells support megakaryocyte and pro-platelet formation from CD34(+) hematopoietic progenitor cells. *J Cell Physiol* 2000;184:58–69.
- Ratajczak J, Zuba-Surma E, Klich I, et al. Hematopoietic differentiation of umbilical cord blood-derived very small embryonic/epiblast-like stem cells. *Leukemia* 2011;25:1278–85.
- Azuma H, Paulk N, Ranade A, et al. Robust expansion of human hepatocytes in Fah^{-/-}/Rag2^{-/-}/Il2rg^{-/-} mice. *Nat Biotechnol* 2007;25:903–10.
- Strick-Marchand H, Dusséaux M, Darche S, et al. A novel mouse model for stable engraftment of a human immune system and human hepatocytes. *PLoS One* 2015;10:e0119820.
- Zhang TY, Yuan Q, Zhao JH, et al. Prolonged suppression of HBV in mice by a novel antibody that targets a unique epitope on hepatitis B surface antigen. *Gut* 2016;65:658–71.
- Yuan L, Liu X, Zhang L, et al. A chimeric humanized mouse model by engrafting the human induced pluripotent stem cell-derived hepatocyte-like cell for the chronic hepatitis B virus infection. *Front Microbiol* 2018;9:908.
- Anthony PP, Ishak KG, Nayak NC, et al. The morphology of cirrhosis: definition, nomenclature, and classification. *Bull World Health Organ* 1977;55:521–40.
- Anthony PP, Ishak KG, Nayak NC, et al. The morphology of cirrhosis: recommendations on definition, nomenclature, and classification by a working group sponsored by the world health organization. *J Clin Pathol* 1978;31:395–414.
- Yanguas SC, Cogliati B, Willebrords J, et al. Experimental models of liver fibrosis. *Arch Toxicol* 2016;90:1025–48.
- Sun S, Li J. Humanized chimeric mouse models of hepatitis B virus infection. *Int J Infect Dis* 2017;59:131–6.
- Gerson SL. Mesenchymal stem cells: no longer second class marrow citizens. *Nat Med* 1999;5:262–4.
- Shultz LD, Ishikawa F, Greiner DL. Humanized mice in translational biomedical research. *Nat Rev Immunol* 2007;7:118–30.
- Shultz LD, Brehm MA, Garcia-Martinez JV, et al. Humanized mice for immune system investigation: progress, promise and challenges. *Nat Rev Immunol* 2012;12:786–98.
- Frenette PS, Pinho S, Lucas D, et al. Mesenchymal stem cell: keystone of the hematopoietic stem cell niche and a stepping-stone for regenerative medicine. *Annu Rev Immunol* 2013;31:285–316.
- Ivanovska IL, Shin JW, Swift J, et al. Stem cell mechanobiology: diverse lessons from bone marrow. *Trends Cell Biol* 2015;25:523–32.
- Xin T, Greco V, Myung P. Hardwiring stem cell communication through tissue structure. *Cell* 2016;164:1212–25.
- Miyajima A, Tanaka M, Itoh T. Stem/progenitor cells in liver development, homeostasis, regeneration, and reprogramming. *Cell Stem Cell* 2014;14:561–74.
- Loomba R, Liang TJ. Hepatitis B reactivation associated with immune suppressive and biological modifier therapies: current concepts, management strategies, and future directions. *Gastroenterology* 2017;152:1297–309.
- Liang TJ, Block TM, McMahon BJ, et al. Present and future therapies of hepatitis B: From discovery to cure. *Hepatology* 2015;62:1893–908.
- Park SH, Rehmann B. Immune responses to HCV and other hepatitis viruses. *Immunity* 2014;40:13–24.
- Billerbeck E, Wolfisberg R, Fahnøe U, et al. Mouse models of acute and chronic hepatitis B virus infection. *Science* 2017;357:204–8.
- Liedtke C, Luedde T, Sauerbruch T, et al. Experimental liver fibrosis research: update on animal models, legal issues and translational aspects. *Fibrogenesis Tissue Repair* 2013;6:19.
- Diggins KE, Greenplate AR, Leelatian N, et al. Characterizing cell subsets using marker enrichment modeling. *Nat Methods* 2017;14:275–8.
- Roussel M, Ferrell PB, Greenplate AR, et al. Mass cytometry deep phenotyping of human mononuclear phagocytes and myeloid-derived suppressor cells from human blood and bone marrow. *J Leukoc Biol* 2017;102:437–47.